Wing Yin Kwong
Institute for Aerospace Studies,
University of Toronto,
Toronto, ON M3H5T6, Canada
e-mail: penelope.kwong@mail.utoronto.ca

Peter Yun Zhang
Department of Mechanical and
Industrial Engineering,
University of Toronto,
Toronto, ON M5S3G8, Canada
e-mail: peteryun.zhang@mail.utoronto.ca

David Romero
Department of Mechanical and
Industrial Engineering,
University of Toronto,
Toronto, ON M5S3G8, Canada
e-mail: d.romero@utoronto.ca

Joaquin Moran
Renewable Power Division,
Hatch, Ltd.,
Niagara Falls, ON L2E7J7, Canada
e-mail: jmoran@hatch.ca

Michael Morgenroth
Renewable Power Division,
Hatch, Ltd.,
Niagara Falls, ON L2E7J7, Canada
e-mail: mmorgenroth@hatch.ca

Cristina Amon
Department of Mechanical and
Industrial Engineering,
University of Toronto,
Toronto, ON M5S3G8, Canada
e-mail: cristina.amon@utoronto.ca

Multi-Objective Wind Farm Layout Optimization Considering Energy Generation and Noise Propagation With NSGA-II

Recently, the environmental impact of wind farms has been receiving increasing attention. As land is more extensively exploited for onshore wind farms, they are more likely to be in proximity with human dwellings, increasing the likelihood of a negative health impact. Noise generation and propagation remain an important concern for wind farm's stakeholders, as compliance with mandatory noise limits is an integral part of the permitting process. In contrast to previous work that included noise only as a design constraint, this work presents continuous-location models for layout optimization that take noise and energy as objective functions, in order to fully characterize the design and performance spaces of the wind farm layout optimization (WFLOP) problem. Based on Jensen's wake model and ISO-9613-2 noise calculations, single- and multi-objective genetic algorithms (GAs) are used to solve the optimization problem. Results from this bi-objective optimization model illustrate the trade-off between energy generation and noise production by identifying several key parts of Pareto frontiers. In particular, it was observed that different regions of a Pareto front correspond to markedly different turbine layouts. The implications of noise regulation policy—in terms of the actual noise limit—on the design of wind farms are discussed, particularly in relation to the entire spectrum of design options.
[DOI: 10.1115/1.4027847]

1 Introduction

Installed capacity for electricity generation from wind has experienced a tremendous increase in the past decade. The Canadian Wind Energy Association envisioned Canada to have 55 GW of wind energy installation by 2025, equivalent to 20% of the country's energy needs [1]. The United States of America has seen sustained, significant growth since 2007, with a verified summer peak generation capacity of 38 GW as of 2010, a total installed nominal capacity of 43 GW through Q3 of 2011 [2], and an additional 15 GW planned for the period 2011–2015 [3]. The latest statistics report that, in 2012, the USA generated electricity from wind at an average rate of 3.8×10^6 MW-h per day during 2012 [3].

Notwithstanding these growing trends, wind energy is still facing resistance in North America due to health and environmental concerns. The government of Canada has published a series of reports regarding noise generation of wind farms [4–6], reflecting increasing public awareness of this potential issue. Although it is still unclear whether wind farm noise has negative health impact, it concerns both the developers and the residents near wind farms. Therefore noise is an important factor in wind farm design.

Noise generation in wind turbines can be generally traced back to either mechanical noise (operation of turbine's mechanical components produces noise) or aerodynamic noise (generated by wind flow and its interaction with the turbine itself). Noise propagation is affected by several factors, including ground effects, topography, temperature, atmospheric conditions, aerodynamic effects caused by wake interactions, and the geometric configuration between noise sources and receivers. Due to the aerodynamic nature of both energy capture and noise generation/propagation, these are usually competing factors, meaning that the more energy captured with a given set of wind turbines due to higher wind speeds, the more noise that might be generated, both mechanically and aerodynamically. An indirect effect also appears when the number of turbines in a given area is increased with the goal of increasing the total energy capture. In such situations, the number of noise sources increases, and the average distance between the turbines and a noise receiver is bound to decrease, thus potentially increasing the sound level measured at the receiver's location.

Traditionally, wind farm design engineers and researchers have considered energy or profit maximization objectives [7,8], and some have included other constraints such as land use, setbacks, and noise limits in their optimization models [9,10]. Hence, feasible solutions in these studies refer to turbine layouts that satisfy all regulatory setbacks, infrastructure and financial constraints, as well as the noise regulations. In other words, when previous works have considered noise as a design factor, they have tried to find

Contributed by the Design Automation Committee of ASME for publication in the Journal of Mechanical Design. Manuscript received January 25, 2013; final manuscript received May 29, 2014; published online July 3, 2014. Assoc. Editor: Michael Kokkolaras.

the wind farm design with maximum energy (or minimum energy cost per unit), while keeping the noise levels below a certain threshold. There are a few potential limitations to this approach. If the design optimization is done manually, as it is typically done in the wind energy industry, wind farm design is an iterative and lengthy process, involving stages of layout design for maximum energy, checks for compliance with environmental restrictions (e.g., noise, setbacks), and refinement of the layout based on infrastructure considerations, potentially leading to suboptimal solutions. Also, feasible solutions might be scarce, if they exist at all, so that it might be challenging to find an acceptable layout. From both the designer's and developer's perspectives, the current design approach fails to elucidate the nature of the energy-noise trade-offs that might be necessary to find an acceptable turbine layout, thus making it difficult to transfer case-specific knowledge to new wind farm projects, and to the WFLOP in general.

In summary, there is a need for a computational approach for optimization of noise-constrained wind farm layouts that is capable of (a) finding the optimal solution, as well as a set of feasible solutions with acceptable performance, (b) elucidating the design energy-noise trade-offs, and the sensitivity of the solution to changes in the preferences of the decision maker toward these different optimization objectives. In the present work, an approach addressing these issues is proposed, considering both noise minimization and energy maximization as potentially conflicting objectives. Following previous works, a stochastic optimization method, namely GAs, is used to solve to identify whether noise and energy generation are truly competing factors; and if so, what the relationship between noise and energy is. In addition, insights are gained by analyzing the populations of solutions generated by the GA, identifying characteristics of layouts that are associated with good performance. In other words, the goal in using this approach is to understand the trade-off between energy and noise in wind farm layout design, and to data-mine the behavior of the algorithm toward convergence with the hope of extracting useful design guidelines.

1.1 Previous Work. Among the recent research work in wind farm design, most relevant to this work are developments in wind farm optimization models and algorithms. In the following, developments on these two aspects are briefly described.

The first study that can be found in WFLOP can be traced back to Mosetti et al. [7], who used a 2.0 km by 2.0 km square to represent the available land. This land was divided into a 10 by 10 grid of square cells, each cell with the side length of five turbine diameters. Turbines could only be placed in the center of a grid cell, thus enforcing design guidelines that prescribe minimum separation distance between turbines. The authors modeled turbine interactions with the Jensen wake model [11], which considers a linearly expanding wake, resulting in a downstream wind speed that is a nonlinear function of downstream distance. As an optimization algorithm, Mosetti et al. [7] used GAs [12], which has been by far the most commonly used method in the literature. Grady [8] further explored GAs as a solution method, using larger populations and number of generations than previous work, thus leading to better solutions. Emami and Noghreh [13] and Serrano-González et al. [14] have further improved over the approach in Ref. [7], the former by including alternative solution encodings and cost functions, and the latter by including a more comprehensive cost model with infrastructure considerations.

More comprehensive models have been proposed recently. Kusiak and Song [15] solved the turbine layout problem with a continuous-location model, in which turbines were allowed to reside anywhere within the wind farm. Minimum turbine proximity and a closed wind farm boundary were imposed as the only constraints, which were then converted into a second objective function. Réthoré et al. [16] explored optimization for offshore wind farms, including an improved cost model in the calculation of the unit cost of energy, which they used as the optimization objective. Saavedra-Moreno et al. [17] incorporated a wind regime that considers spatial difference in wind speeds. In other words, instead of using a single wind speed/direction or a distribution of wind speed and directions for the whole farm terrain, their model considers the spatial distribution of the wind resource within the farm. Réthoré et al. [16] also used the discrete-location approach. However, they employed a two-stage model with increasing resolution of the wind farm. In the second stage, the authors also included more comprehensive cost and revenue models, and increased the number of directions and speeds for wind resources. Chowdhury et al. [10,18] investigated how land configuration influenced the wind farm's performance. Finally, other recent developments on the modeling side are the work of Serrano-González et al. [14], who include infrastructure considerations in the layout design, such as the cost of foundations and the cost of auxiliary inner roads connecting turbines, and Şişbot et al. [19], who included an improved cost model and solved the WFLOP with a multiobjective GA using energy and cost as optimization objectives.

On the algorithmic side of the problem, different methods have been explored. Stochastic metaheuristics such as GAs and Particle Swarm Optimization [20] have been extensively applied to the wind farm optimization problem [7,8,21,22] with success. Deterministic heuristics have also been used, such as the extended pattern search (EPS) approach of Du Pont and Cagan [23,24]. In EPS, each turbine in the layout is moved according to a preestablished pattern, with a step size that decreases as the optimization progresses. Turbine moves that lead to an increase in energy production are kept, while those that do not are discarded. This heuristic strategy's rejection-sampling approach is guaranteed to improve upon the initial solution, although there are no guarantees of global convergence.

An alternative approach for the solution of the WFLOP is that proposed by Donovan [25,26] and Fagerfjäll [9], who explored mixed-integer programming (MIP) models, and solved these problems with traditional branch-and-bound methods. Unlike GAs and other heuristics, MIP solvers are included in many software packages for operations research, e.g., IBM ILOG CPLEX [27], and have well-studied convergence behaviors. However, these solvers are not always suited for nonlinear, nonconvex optimization problems, as the WFLOP is. In fact, both Donovan and Fagerfjäll used an approximate, simplified calculation of energy capture in order to justify their use of linear MIP solvers on what is a fundamentally nonlinear problem. More recent contributions that do not rely on simplified wake modeling are those of Turner et al. [28] and Zhang et al. [29].

On a broader scope, the authors intend to solve the full-scale, comprehensive WFLOP problem, including major aspects of the problem: Energy capture, environmental impact and cost. As a first step toward that vision, this paper focuses on understanding the energy-noise trade-off in wind farm layout design. The remainder of this paper is organized as follows. In Sec. 2, the models that are used to predict energy capture and noise generation/propagation in the wind farm are described. Then, a brief description of the optimization method used in this work (NSGA-II) is presented, followed by the test cases and the results of a comparison study with respect to open source, industry-grade software for computer-aided wind farm design. Finally, single- and multiobjective optimization (MOO) results are presented and discussed, followed by concluding remarks and some ideas for future work.

2 Wind Farm Modeling

2.1 Wake Modeling. An analytical, closed-form wake model is used to quantify the aerodynamic interaction between turbines. This model was first proposed by Jensen [11], who developed it by considering that momentum is conserved within the wake, and that the wake region expands linearly in the direction of the flow, as shown in Fig. 1.

To determine the effective wind speed experienced by a turbine located within another turbines wake, the momentum balance equation is written, i.e.,

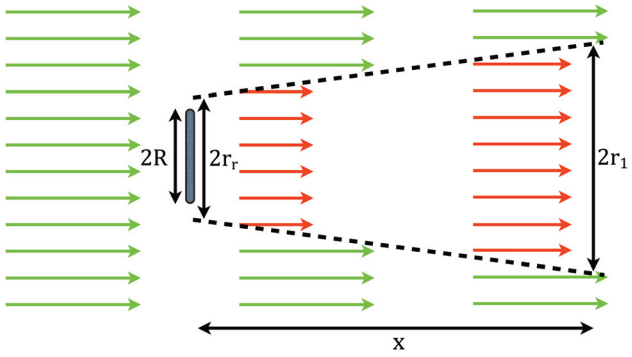

Fig. 1 Schematic representation of Jensen's wake model

$$\pi r_r^2 u_r + \pi\left(r_1^2 - r_r^2\right)u_o = \pi r_1^2 u \tag{1}$$

where r_r is the wake radius immediately after the turbine, r_1 is the radius of the wake at any position x measured downstream, u_o is the free stream wind speed, u_r is the wind speed immediately behind the rotor, and u is the speed of wake a downstream distance x.

According to Betz's theory [30], the wind speed immediately behind the rotor is approximately 1/3 of the free stream speed, and with the assumption of a linearly expanding wake, the downstream speed can be calculated as

$$u = u_o\left(1 - \frac{2}{3}\left(\frac{r_r}{r_1}\right)^2\right) \tag{2}$$

where $r_1 = r_r + \alpha x$, and α is the entrainment constant, also known as the wake decay constant

$$\alpha = \frac{0.5}{\ln\left(\frac{z}{z_o}\right)} \tag{3}$$

where z is the hub height and z_o is the surface roughness of the terrain, both in meters. Figure 2 shows the variation of wind speed downstream of a turbine as a function of position along the wake's centerline. Note the nature of the decay in wind speed, and the rate at which it recovers its free stream value. This behavior is relevant in understanding the WFLOP, as it indicates that layouts in which the turbines are as far apart as possible are preferred. For turbines under the influence of multiple wakes, an effective wind speed can be calculated from the sum of kinetic energy deficits from upstream turbines. This approach has been used extensively in previous work, especially for optimization purposes, and it is still used in commercial software for wind farm design. For more complex models of wake dynamics, the reader can refer to Ref. [31]. The effective speed of a turbine inside n wake regions can therefore be expressed as

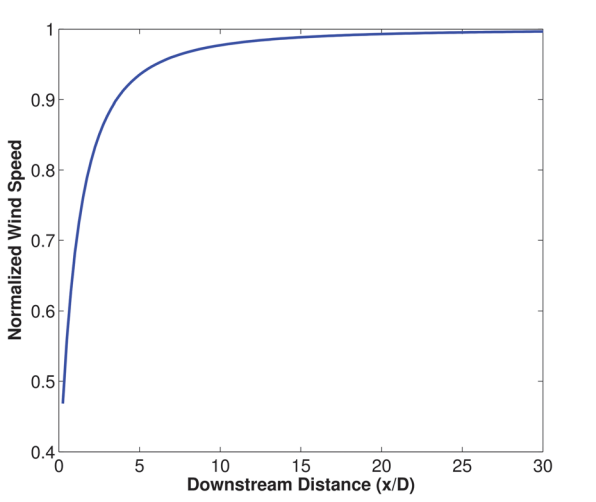

Fig. 2 Wind speed along a single wake's centerline, as a function of distance normalized with the turbine diameter ($z = 60$ m, $z_o = 0.3$ m, $R = 20$ m, and $C_t = 0.88$)

$$u(x) = u_o\left[1 - \sqrt{\sum_{i=1}^{n}\left(1 - \frac{u_i(x)}{u_o}\right)^2}\right] \tag{4}$$

Based on the effective wind speed at the turbine rotor, the power produced by the turbine can be calculated through the manufacturer-supplied power curve. Without loss of generality, the present work mirrors previous work and uses a simplified expression for a turbine's power output, in which power is a simple cubic function of the local effective speed at hub height. Hence, when the farm is subjected to a uniform wind speed, the total power extracted from k wind turbines is expressed in the following equation [7,8,24]:

$$P_{\text{tot}} = \sum_{i=1}^{k}\frac{1}{3}u_i^3 \tag{5}$$

Finally, note that the annual energy production (AEP), expressed in (kW-h) of a wind farm is defined as the integration of power (kW) over time (h). In the general case, this is an expected value of a random variable, as it is based on the probability distribution of wind speeds and directions. Hence, it is calculated as

$$\text{AEP} = 8766\sum_{i=1}^{k}\sum_{d\in\mathcal{D}}\frac{1}{3}u_{id}^3 p_d \tag{6}$$

where u_{id} is the effective wind speed at turbine i at hub height for wind state d, i is an index over the number of turbines k, $d \in \mathcal{D}$ is the set of all possible wind states (i.e., the set of all possible wind speeds and directions), p_d is the probability of wind being at state d, and 8766 is the effective number of hours in a year.

2.2 Noise Modeling. In the context of the ISO-9613-2 standard [32], receptors are the locations where the sound level is to be measured or predicted. In wind farm layout design, all residences located within the wind farm terrain, or within a certain jurisdiction-dependent neighborhood, are considered receptors for noise calculation purposes.

In a practical setting, the equivalent continuous downwind octave-band sound pressure level (SPL) at each receptor location is calculated for each point source, at each of the eight octave bands with nominal midband frequencies from 63 Hz to 8 kHz [32], as

$$L_f = L_{\text{w}} + D_{\text{c}} - A \tag{7}$$

where L_{w} is the octave-band sound power emitted by the source, D_{c} is the directivity correction for sources that are not omnidirectional, A is the octave-band attenuation, and subscript f indicating that this quantity is calculated for each octave band frequency.

Several octave-band weightings are available to convert the SPLs in Eq. (7) to an effective SPL. For wind farm layout applications, it is customary to use A-weighted SPLs [5]. The equivalent continuous A-weighted downwind SPL at specific location can be calculated from summation of contributions of each point sound source at each octave band

$$L_{\text{avg}} = 10\log\left(\sum_{i=1}^{n_s}\left(\sum_{j=1}^{8} 10^{0.1\left(L_f(i,j)+A_f(j)\right)}\right)\right) \tag{8}$$

where n_s is the number of point sound sources, j is the index representing one of the eight standard octave-band midband frequencies, and the $A_f(j)$ are the standard A-weighting coefficients.

The attenuation term (A) in Eq. (7)

$$A = A_{\text{div}} + A_{\text{atm}} + A_{\text{gr}} + A_{\text{bar}} + A_{\text{misc}} \tag{9}$$

is the sum of different attenuation effects due to geometrical divergence (A_{div}), atmospheric absorption (A_{atm}), ground effects (A_{gr}), sound barriers (A_{bar}), and miscellaneous effects (A_{misc}). In this model, it is assumed that the attenuation due to sound barriers and miscellaneous effects are negligible. Further detail of the calculation procedure can be found in the ISO 9613-2 document [32]. An illustration of the behavior of the SPL as a function of (radial) distance with respect to the source is shown in Fig. 3. Note that this behavior is opposite to the speed recovery shown in Fig. 2. The implication for the layout designer is that turbines, when seen as noise sources, should be located as far away as possible from the receptors. This guideline might conflict with the previous one stating that turbines should be as far away from each other as possible, resulting in the noise-energy trade-off described in the present work.

It is important to note that the ISO-9613-2 model does not include any provisions for modeling the effects of wind speed and direction on noise propagation, among other simplifying assumptions made in its development. More sophisticated noise modeling approaches are available [33] that exhibit enhanced spectral resolution and accurate handling of complex meteorological conditions. A specific example is the NORD2000 model [33], which has been validated for noise predictions in wind farms located in complex terrains, and has shown good accuracy in predicting both the sound power level and its frequency spectra [34]. In the present work, however, we adhere to the ISO-9613-2 standard as the method most commonly used by industry, and also because it is sufficient for our present noise modeling needs, which involve wind farms in flat terrains, without sound barriers, and simple wind regimes, conditions which fall within the domain of validity of the ISO-9613-2 noise propagation model.

3 Optimization With GAs

In this work, the energy/noise, multi-objective WFLOP is defined as

$$\underset{\boldsymbol{x}_t}{\text{minimize}} \quad \left(-\text{AEP}(\boldsymbol{x}_t), \text{SPL}(\boldsymbol{x}_t)\right) \tag{10}$$

with

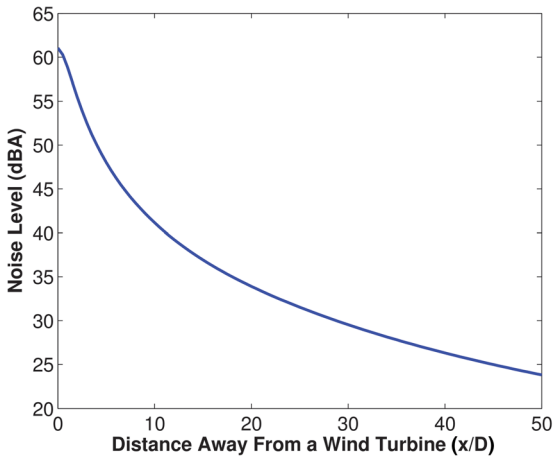

Fig. 3 SPL (*A*-weighted) as a function of distance from the source (L_{wA} = 100 dBA, D_c = 0, receptor height h_r = 1.5 m)

$$\text{AEP}(\boldsymbol{x}_t) = \sum_{i=1}^{k}\sum_{d\in\mathcal{D}}\frac{1}{3}\left(u_{id,\infty}\left[1-\sqrt{\sum_{j\in\mathcal{U}_{id}}\left(1-\frac{u_{ijd}}{u_{id,\infty}}\right)^2}\right]\right)^3 p_d$$

and

$$\text{SPL}(\boldsymbol{x}_t;\boldsymbol{x}_r) = 10\log\left(\sum_{i=1}^{k}\sum_{j=1}^{8} 10^{0.1\left(L_f^{(i,j)}(\boldsymbol{x}_t;\boldsymbol{x}_r)+A_f^{(j)}\right)}\right)$$

where $\boldsymbol{x}_t$ is a continuous vector containing the coordinates of the k turbines to be placed, $\boldsymbol{x}_r$ is the vector of coordinates of the noise receptors, $\mathcal{U}_{id}$ is the set of turbines that are upstream of turbine i for wind state d, $u_{id,\infty}$ is the undisturbed wind speed at turbine i for wind state d, and u_{ijd} is the wind speed at turbine i due to a single wake caused by upstream turbine j for wind state d. Note that neither equality nor inequality constraints have been included in this problem, as the present work focuses on using MOO as a tool to study the problem characteristics, particularly the energy-noise trade-off.

In this work, GAs [12] are used to solve the multi-objective WFLOP in Eq. (10). GAs are probabilistic search algorithms inspired by the concept of natural selection and survival of the fittest. GAs search through the solution space by keeping a population (set) of solutions, which are ranked according to their fitness to solve the optimization problem (e.g., objective function values), and evolved through many generations. Due to their probabilistic nature, GAs are complete search methods, meaning that they can perform an exhaustive search of the input space if they are run for long enough, as long as the elitism, cross-over and mutation operators are implemented with nonzero probability [35]. In other words, GAs are guaranteed to converge to the neighborhood of the global optima, but they can take an arbitrarily large number of function evaluations (i.e., run time) to do so.

An important advantage of GAs is that they do not require information about the gradient of the solutions, therefore avoiding problems with the nonconvexity and noncontinuity of the solution space. This characteristic of GAs makes them well suited for the WFLOP. On the other hand, GAs typically exhibit slow rates of convergence, thus increasing the computation cost and runtime of the optimization. This work will not focus on improving the runtime behavior and/or convergence rate of the algorithm. Rather, it will exploit its advantages to characterize the design space of the wind farm layout.

Because they are population-based optimization method, GAs are particularly well suited for MOO problems, and several variants of GAs have been proposed for MOOs, such as the strength-Pareto evolutionary algorithm (SPEA, SPEA-2) [36,37], and the nondomination sorting genetic algorithm (NSGA, NSGA-II) [38,39], among others [40]. Both SPEA-2 and NSGA-II assign a rank to each member of the population based on the Pareto dominance concept, hence they do not require weighting the objective function values to order/rank the population of solutions uniquely. It is worth mentioning that SPEA-2 and NSGA-II have been shown to have similar performance over an array of test functions. This is expected since the algorithms are very similar, the main difference being the method used to convert multiple objective function values to a unique metric of fitness.

The NSGA-II algorithm, which is based on two fitness metrics, i.e., nondomination sorting/ranking and crowding distance, is used in the present work. First, in the nondomination sort stage, a candidate solution is assigned an integer fitness value that indicates its rank in the population, according to the Pareto dominance criterion. In other words, solutions that are part of the nondominated front are assigned a rank value of 1, solutions that would be part of the nondominated front if rank 1 solutions were removed are assigned a rank value of 2, and the process is repeated until all solutions in the current population have been assigned a rank. Second, a crowding distance metric is calculated for every solution,

defined as the distance between the solution and it is nearest equally ranked neighbor in the objective space. This second metric is used to maintain certain diversity in the population, a characteristic that has been found important for convergence to the global optima [39]. In the following paragraph, a step by step description of the NSGA-II algorithm is presented, in the context of the WFLOP.

In the WFLOP, n_{pop} initial layout patterns are generated randomly, and the corresponding objective values (energy generation, sound pressure level) are evaluated. For each individual in the population, a rank is assigned according to their nondomination status and the distance between the solution and its neighbors in the objective space. In the parent selection stage, parents for the next generation are chosen based on the rank and the crowding distance via binary tournament. Solutions with lower rank values are preferred, as the ranks are assigned so that the current Pareto front has rank 1. Crowding distance is used as a secondary fitness value to break ties when comparing solutions based on rank. After parents are selected, an offspring generation of size n_{off} is created by cross-over and mutation of the layout patterns of the parent generation. After evaluating the objective function values of the offspring population, it is merged with the parent population, and new rank and crowding distance values are assigned. Elitism is implemented by keeping only the best (i.e., rank 1) or the first n_{pop}-best solutions for the next generation (iteration) of the algorithm. The readers are referred to Ref. [39] for more details on the NSGA-II algorithm and its implementation.

To evaluate whether the algorithm has converged, a variety of criteria could be used. Besides monitoring changes in the nondominated hyper-volume (NDHV) across generations, this work implements the approach of Deb et al. [39], which determines convergence by monitoring the change in crowding distances across 200 generations. This convergence criterion was uniformly applied when generating all results included in the paper.

4 Test Cases

For consistency with previous work, this work uses the same test cases that are typically reported in the WFLOP literature. A square wind farm terrain, of size 2 km × 2 km is considered. In this farm, a fixed, given number of identical turbines is to be placed, with turbine parameters as defined in Table 1. Two wind regimes, WR1 and WR36, which are tested separately, are assumed to be uniform over the wind farm terrain, without loss of generality. The first one (WR1) has a uniform, single-direction wind pointing from south to north at 12 m/s, while the latter (WR36) includes a nonuniform probability distribution for wind coming from 36 directions with three different speeds, as described by Fig. 4, which is mirrored from previous work [8,24]. Figure 5 illustrates the wind farm terrain with seven turbines under WR1. It is important to note that the choices of test cases, wind resource and wind turbine characteristics such as rotor diameter, hub height, power curve and thrust coefficient curve, are not expected to have a significant effect on the mathematical behavior of the multi-objective problem. In other words, these choices are expected to affect the quantitative predictions of SPL and AEP,

Table 1 Wind turbine parameters used for the case studies [7,8,14]. Reference [24] used the same parameters, with the exception of $z_o = 0.5$ m.

Parameter	Value
Turbine hub height (z)	60 m
Terrain roughness length (z_o)	0.3 m
Rotor radius (r_r)	40 m
Thrust coefficient (C_T)	0.88
Power curve	$0.3u^3$ kW
Noise generation (L_{wA})	100 dBA
Noise receiver height (h_r)	1.5 m

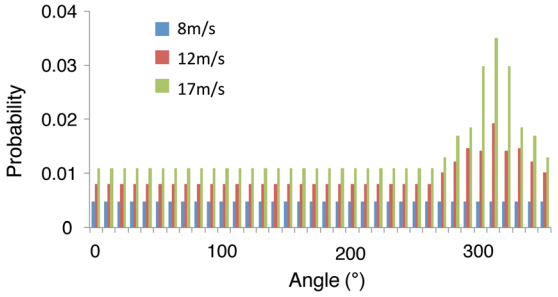

Fig. 4 Distribution of wind speeds and directions for WR36 cases [8,24]

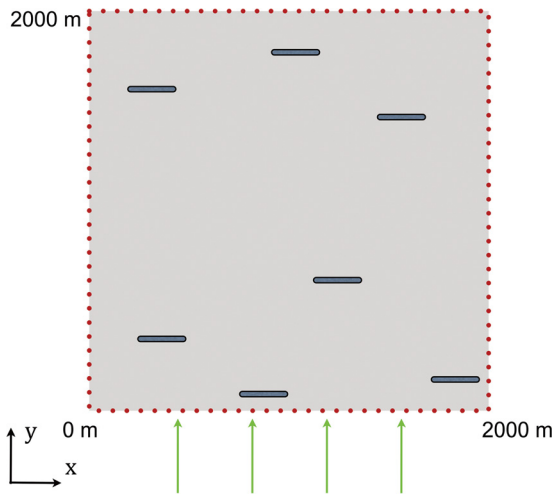

Fig. 5 Schematic representation of a test case. Seven turbines are shown facing the wind direction. Noise receptors, represented by dots, are located along the edges of the wind farm every 50 m.

but not necessarily the overall nature of their functional dependence on the turbine coordinates, see Sec. 5.4 for an illustration of the impact of these modeling choices. Note also that the optimization problem is defined as finding the best location of a given number of turbines, as indicated in Eq. (10). In the results shown below, this problem is solved repeatedly, each problem instance corresponding to a different number of turbines.

In previous studies, proximity constraints were enforced on the turbines, either directly as inequality constraints restricting the distance between any pair of turbines to be larger than five times the turbine diameter (5D), or indirectly by using a discrete formulation of the WFLOP with a cell size defined to enforce this 5*D* rule. In the present work, turbine positions are allowed to vary continuously, to more closely reflect the setting found in layout design practice. Note that turbine proximity constraints are not enforced during the optimization, to allow them to arise naturally from the optimization objectives. Analysis of our results, not included in this paper for the sake of conciseness, indicated that unconstrained Pareto-optimal solutions commonly have a few turbines violating the proximity constraints, although this is not always the case.

Section 5 presents the results of the optimization study. First, a comparison of the energy and noise models, as implemented in the present work, was conducted by comparing their results both with previous work and with an industry-grade, open-source software for computer-aided wind farm design and analysis, OPENWIND [41]. Then, the trade-off surface for the multi-objective, energy-noise optimization is presented and discussed, along with the potential implications for wind farm layout design practice.

Table 2 Comparison of AEP predictions between the present work and OPENWIND [41], 3 km × 3 km wind farm, using the piecewise-linear power curve and second wind scenario from Ref. [15], herein referred to as W24-V

No. of turbines	Wind regime	Current study (GW h)	OPENWIND (GW h)	% Diff.
30	WR1	132.38	132.17	0.16
30	WR36	225.88	230.48	1.99
10	W24-V	40.96	42.20	2.94
20	W24-V	80.89	82.71	2.20
30	W24-V	114.47	116.97	2.14
40	W24-V	150.72	155.48	3.06
50	W24-V	174.74	181.95	3.96

5 Results and Discussion

5.1 Comparative Verification of the Models. The first task in the optimization effort was the implementation of the wake and noise models for evaluating the performance of a wind farm. The C++ programming language was chosen for this task for its computational efficiency. To verify the implementation, the AEP and SPL was calculated for several random, nonoptimal layouts with different numbers of turbines, from 10 to 50, using (a) the present implementation of the models, (b) OPENWIND [41]. For this comparison study, a realistic wind regime (denoted W24-V) obtained from Kusiak and Song [15] was used. This wind regime specifies the wind resource over 24 angular sectors by a set of Weibull parameters (shape, scale) and a probability for each sector. Two additional tests cases with 30 turbines were also run, using the wind regimes WR1 and WR36, which have been used frequently in previous research on the WFLOP. Table 2 shows the predicted energy performance according to these models, and their difference expressed as a percentage of the OPENWIND prediction, which is reported to have been thoroughly compared [42] against WINDPRO, one of the *de facto* industry standards for computer-aided wind energy engineering. As an illustration, Figs. 6 and 7 allow comparing the predicted SPLs inside the wind farm terrain for the WR36 case with 30 turbines. After noting the slight difference in color map, legend, and scale, it can be seen that the predictions are similar.

5.2 Energy Maximization. As a second step in the verification of our implementations, single-objective optimization studies were conducted to maximize the energy production of the wind farm. The rationale for this study is to ensure that, when using the present implementations of the wake models in combination with a GA implementation, results comparable to those reported in previous work are obtained. This is motivated by the reported discrepancy in results obtained by different researchers across the same set of test cases [7,8,15,23,24], each time requiring a re-evaluation of the results to ensure a fair comparison. It is important to note that, although NSGA-II was not specifically designed for single-objective optimization, it is guaranteed to work in such settings, because it is equivalent to a traditional GA in which the fitness values of the population are generated by a monotonic rank-transformation of the objective function values. At the price of a small impact on the computational efficiency of our code, the authors decided to use this approach since, in the envisioned practical applications, the users would benefit from a single algorithm and implementation that can transparently deal with single-objective optimization and MOO tasks without further user input.

Tables 3 and 4 present the results from the energy optimization runs (with NSGA-II used for single objective), alongside several results from previous work that have used the same problem setup; these have also been re-evaluated using our implementation of the wake models to ensure a fair comparison of the results. In this table, efficiency is defined as the ratio between the total AEP and the total energy that would have been produced without any wake effects. Note that, for computational efficiency and ease of implementation, the present work uses a discrete method to approximate the influence of partial wake effects: if the wake region covers more than 50% of the downstream rotor, the wake is considered to be full-fledged (as if the downstream turbine is entirely in the wake), otherwise it is considered that the downstream rotor is not affected. More comprehensive implementations of the

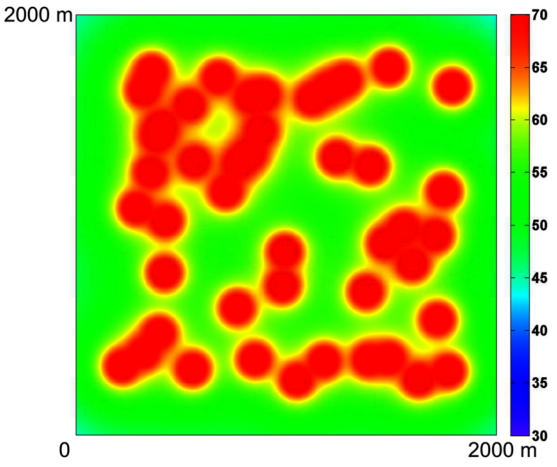

Fig. 6 Sound pressure level contour maps generated by this work's implementation of the ISO-9613-2 standard [32]. Noise values are expressed in (dBA).

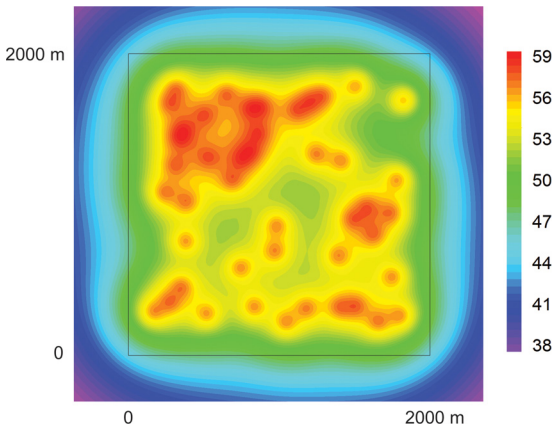

Fig. 7 Sound pressure level contour maps generated by OPENWIND [41]. The black-box indicates the 2 km × 2 km wind farm area, for easier comparison with Fig. 6. Noise values are expressed in (dBA).

Table 3 Comparison of AEP efficiency (%): current study, Grady [8], and Du Pont and Cagan [23], WR1. Layouts from previous work have been re-evaluated using the discrete partial wake approach used in the present work.

	Wind farm efficiency (%)			AEP (GW h)
No. of turbines	Current	Grady	Du Pont	Current
15	99.79	—	—	68.1
20	98.98	—	—	90.8
25	98.14	—	—	113.1
30	91.77	95.13	88.35	134.5
35	91.16	—	—	155.9
39	92.29	—	—	172.1
40	93.05	—	—	177.0
45	88.51	—	—	196.5

Table 4 Comparison of AEP efficiency (%): current study, Mosetti et al. [7], Grady [8], and Du Pont and Cagan [23], WR36. Note that the AEP values reported correspond to the optimal energy solutions shown in Figs. 10 and 11. Layouts from previous work have been re-evaluated using the discrete partial wake approach used in the present work.

	Wind farm efficiency (%)				AEP (GW h)
No. of turbines	Current	Mosetti	Grady	Du Pont	Current
15	96.58	96.69	—	94.51	118.5
20	95.37	—	—	—	156.4
25	93.78	—	—	—	192.4
30	91.87	—	—	—	227.2
35	90.53	—	—	—	262.7
39	88.55	—	89.85	89.39	289.5
40	89.09	—	—	—	296.0
45	88.16	—	—	—	327.9

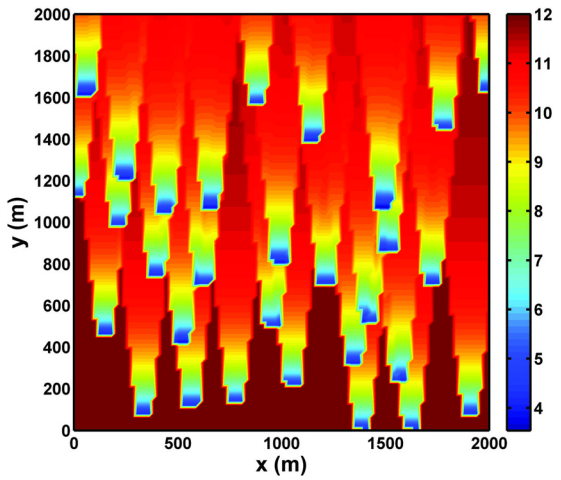

Fig. 8 Predicted wind speed field for DuPont and Cagan's optimal 30-turbine layout (based on Fig. 9 in Ref. [24]), WR1 test case, $z_o = 0.5$ m. Wind speed values are expressed in (m/s).

Jensen wake model accounting for partial wakes can be found in the works of Archer et al. [43], Du Pont and Cagan [23,24,44], Chowdhury et al. [18,45], Gonzalez Rodriguez and coworkers [14], and among others. It is expected that the simplified wake calculation used in the present work will not affect significantly its findings, as the goals of the study focus on characterizing the energy-noise trade-off in wind farm layout design, rather than on obtaining the most accurate wake predictions, especially for the simple test cases used in this work. Although this is probably the cause of small inconsistencies between our re-evaluation of the energy production from previous studies' optimal layouts and their reported results, other differences cannot be explained by this modeling choice. For example, Du Pont and Cagan [23,24] reported an efficiency of 100% for their 30-turbine optimal layout under WR1, while the present work found it to be 88.35%. Figure 8 shows the predicted flow field for this test case, clearly indicating that the efficiency of this layout cannot be 100%, as claimed by the authors (refer to Table 3 in Ref. [24]). Note also the difference between our predicted efficiency for the optimal layout obtained in this work and that of our own re-evaluation of Grady's layout. The main reason for this difference is that the GA did not converge to the global optimum for the 30 turbine case even after repeated runs, while Grady's layout can be considered to be optimal according to our intuition about the problem. In related work we have conducted in our group, we have seen that problem instances requiring placement of 30–40 turbines in the $2\,\text{km} \times 2\,\text{km}$ wind farm are harder to solve that problem instances with smaller or larger numbers of turbines on the same land [28]. There is related literature in the operations research community, referring to the p-dispersion and maximum diversity problems, which also exhibit this behavior. We believe this is the underlying cause for the difficulty in accurately obtaining the global solutions for this subset of test cases.

5.3 MOO. Once the models were fully verified, the MOO study was conducted. The NSGA-II GA was used to solve the problem formulated in Eq. (10). A population size of $4k$ was evolved for a maximum of $200\sqrt{2k}$ generations, where k is the number of turbines to be placed [8], with probabilities for cross-over and mutation of 0.95 and 0.05, respectively. To control for the inherent randomness of the optimization method, each problem instance was solved 10 times. Figure 9 shows an example of the observed convergence curves based on the NDHV for the cases with 39 and 40 turbines. Note that in both cases there are several runs that converged before reaching the maximum number of generations, according to the convergence criteria discussed at the end of Sec. 3.

Figures 10 and 11 show the (approximate) Pareto frontiers for WR1 and WR36 cases, respectively. Each point in the graphs corresponds to one layout, and its coordinates indicate its energy and

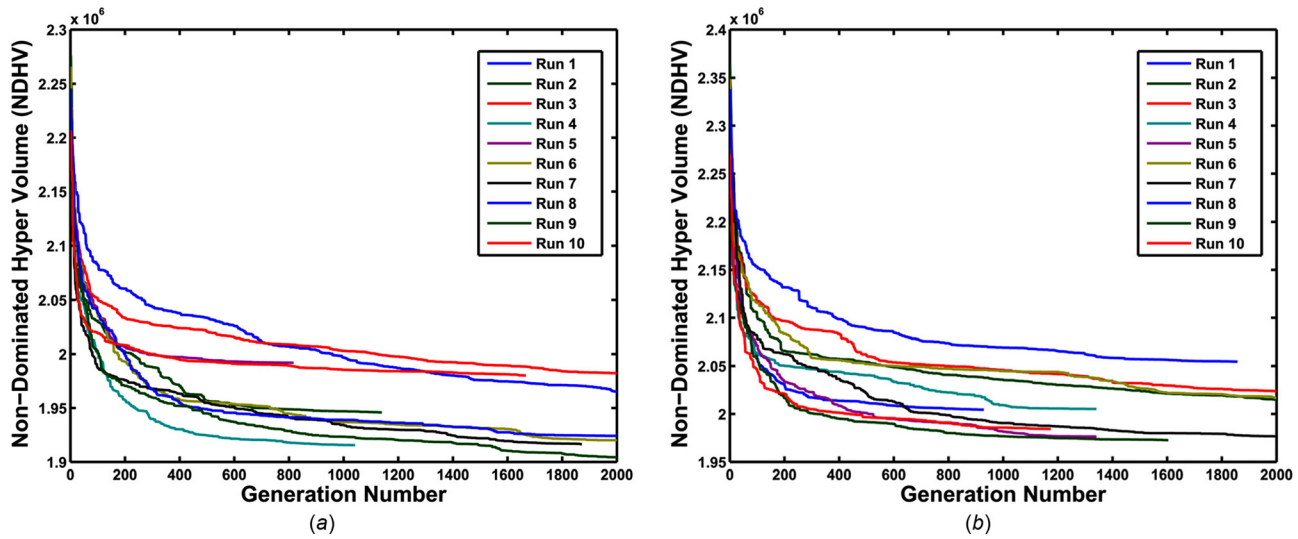

Fig. 9 Convergence of the NDHV of the Pareto front during multiple runs of the NSGA-II multi-objective GA, for cases with (*a*) 39-turbines and (*b*) 40-turbines

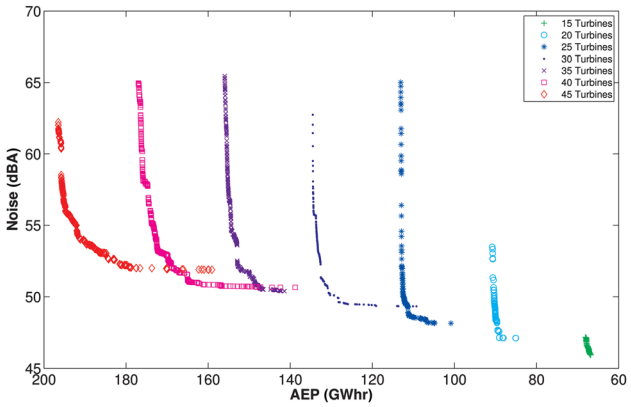

Fig. 10 Pareto frontiers for the WR1 cases. Note that the horizontal axis is reversed.

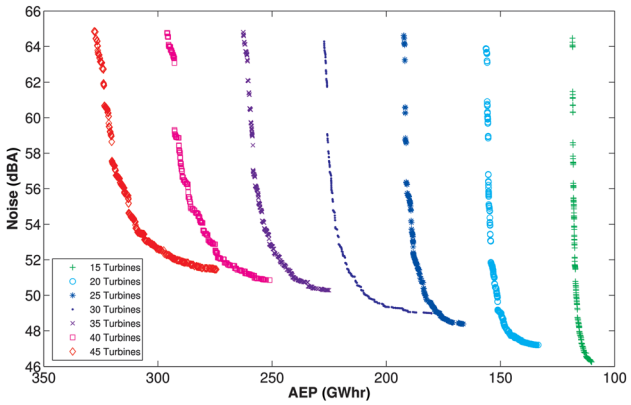

Fig. 11 Pareto frontiers for the WR36 cases. Note that the horizontal axis is reversed.

noise performance. In the WFLOP studied in this work, maximum energy production and minimum noise propagation are indeed competing objectives, as seen by the general trend of increasing sound pressure level with increasing energy production, for a certain number of turbines. This is an interesting fact about the problem nature, and it supports the use of the Pareto Front as means to convey this information to wind farm designers.

There are several important observations about the results presented in Pareto fronts, Figs. 10 and 11. First, note the topmost/leftmost part of the figures, points in this region correspond to layouts that have strong energy performance (the horizontal axis is reversed). Not surprisingly, the maximum amount of energy achievable increases monotonically as a function of total number of turbines. In addition, by comparing the relative distances of the points in the horizontal axes, it can be noted that, for the numbers of turbines studied, each additional turbine adds approximately the same amount of energy output for the optimal solution. This trend is expected to change, however, resulting in Pareto fronts that are closer to each other as the number of turbines in the farm increases further.

Another implication of the Pareto fronts of Figs. 10 and 11 is the wide diversity of layouts that can achieve a given range of energy outputs. For example, consider that Pareto front for a wind farm with 35 turbines under the WR1 wind regime, Fig. 10. The almost vertical section of the Pareto front, consisting of solutions with AEP $>$ 150 GW h, indicates that energy outputs in this range can be achieved with a wide variety of noise levels. In other words, there is a part of the solution space for which the strength of the energy-noise trade-off decreases. This behavior, observed across all test cases with different numbers of turbines and under different wind regimes, is reassuring from the point of view of design practice, as it gives flexibility to the designers in achieving their design objectives.

Regarding sound generation and propagation, it can be observed in the top part of the Pareto fronts that, regardless of the number of turbines, the maximum sound pressure level observed in these tests is approximately 65 dBA. This behavior is expected to change as even more turbines are added to the farm, which will inevitably lead to layouts in which turbines are very close to the wind farm boundaries where the noise receptors are located, resulting in sound pressure levels larger than 65 dBA. In addition, the bottom right of Fig. 11 shows a monotonic increase in the minimum sound levels that are achievable for a given number of turbines. This stresses the importance of sound level regulations in the feasibility of wind development on a given site. As an illustration of this point, under the assumption that there are financial resources available and that there is enough capacity in the electrical distribution network to which the wind farm is connected, it is easy to see that enforcing a maximum sound pressure level of 50 dBA through policy would result in a hard constraint on the maximum attainable AEP. In the specific case of Fig. 11, it can be seen that a 50 dBA noise limit would constrain AEP to approximately 200 GW h. However, a slight relaxation of the regulation, e.g., to 52 dBA, would enable a near 50% increase in AEP to approximately 300 GW h.

A final observation about Figs. 10 and 11 are the intersections between Pareto fronts for different numbers of turbines, see for example the cases with 35, 40, and 45 turbines under WR1, Fig. 10, or a direct comparison of cases with 39 and 40 turbines, Fig. 12. These intersection points represent performance conditions that can be achieved with different numbers of turbines and, conceivably, with different layouts. This is illustrated more clearly in Fig. 13, which shows four layouts that result in approximately the same levels of noise and energy (refer to Fig. 12), but they do so with 39 and 40 turbines. Obviously, economics would favor the layouts with 39 turbines if capital investment is the main consideration.

5.4 Effect of Assumptions on the Pareto Fronts. Figure 14 shows the effect that changes in some of the modeling choices have on the resulting Pareto fronts. Figure 14(*a*) compares the results of the optimization of a 15-turbine layout on a 3 km $\times$ 3 km wind farm under the W24-V wind regime, based on a constant thrust coefficient (see Table 1) and based on a realistic thrust coefficient curve corresponding to a Vestas V63 turbine [46], using the actual power curve from the turbine in both cases. In Fig. 14(*a*), it can be noted that the characteristic trade-off curves are not significantly affected by the thrust coefficient variation, except for a slight change in the maximum attainable AEP values, which increased up to 1%.

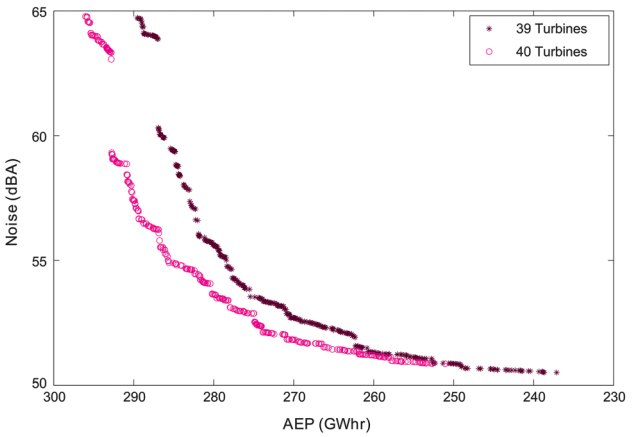

Fig. 12 Pareto frontiers for 39 - and 40-turbine layouts (WR36)

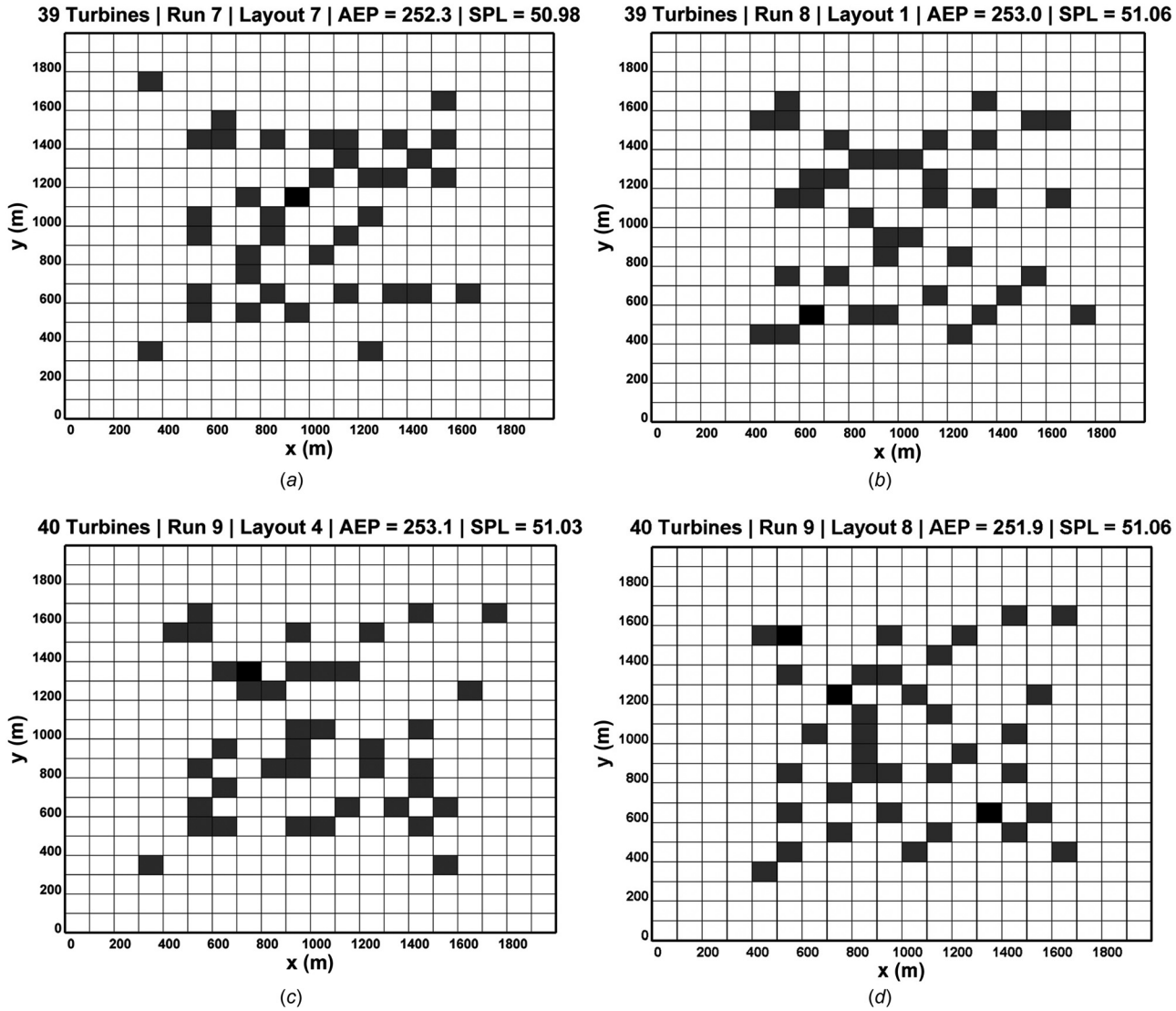

Fig. 13 Alternative layouts with similar performance for 39 and 40 turbines, WR36, 2 km × 2 km wind farm, AEP ≃ 252.5 GW h, SPL ≃ 50.88 dBA

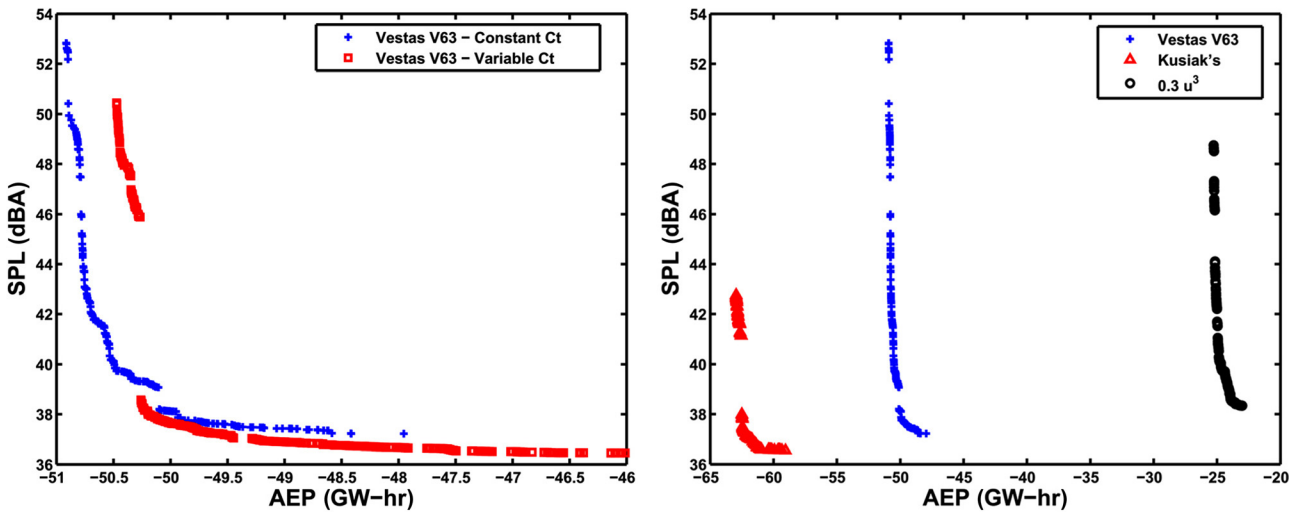

Fig. 14 Effect of modeling simplifications on energy-noise Pareto fronts, 15 turbines, 3 km × 3 km wind farm, W24-V wind regime [15]. Note the difference in scale in the horizontal axes.

On the other hand, changes in the power response of the wind turbines have a very significant effect on the predicted AEP values. Figure 14(*b*) compares the optimization results of the same 15-turbine test case, which was solved three times with different power curves, but assuming a constant thrust coefficient. Note that the differences in AEP between different cases may reach more that 100%, with the ideal power curve $0.3u^3$ yielding the lowest AEP values. However, it is important to note that for all three power curves, the Pareto fronts describe an energy-noise trade-off. This observation corroborates our working assumption that the simple models used in this work are sufficient to describe the energy-noise trade-offs in WFLOP. More realistic application scenarios would undoubtedly rely on more accurate wake models and manufacturer-supplied turbine performance data, as well as more sophisticated noise models such as NORD2000.

6 Conclusion

In this work, a multi-objective formulation for the WFLOP has been presented, which for the first time focuses on both energy and noise as objectives. Instead of focusing on energy-maximization or cost-minimization objectives, the formulation is based on maximizing energy production while minimizing sound levels at the boundary of the wind farm, to more closely resemble the design problem faced by wind farm engineers in industrial practice.

A verification study of the present implementation of wake models has been conducted by the authors, comparing single-objective energy maximization results with previous works, as well as with OPENWIND, an industry-grade software. For the computational implementation of the ISO standard for noise propagation, the verification study relied only on a comparison with OPENWIND, since the present work is the first that considers noise propagation as an objective for WFLOP.

The MOO results discussed in this work characterize the behavior of the WFLOP, and this insight is presented here using a set of Pareto fronts for the energy/noise objectives. The implications of the observed energy-noise trade-off have been discussed. In particular, there is a zone of the Pareto fronts, located toward higher energy values, that guarantees the availability of a wide array of layouts that can meet energy objectives while varying significantly in their noise emissions. On the other hand, the zone of the Pareto front located toward low noise values illustrates how sensitive the optimization problem is to small changes in the allowed noise emission limits. As an example, for the test case used in this work, a relaxation of only 2 dBA in the noise limit would allow for an increase of 50% in the energy production without increasing the number of turbines in the farm. Of course, such analysis would only be valid on a case-by-case basis, as the location of the noise receivers is case-dependent, but the results do show the importance of this type of analysis for wind farm design and public policy.

There are several natural directions for future studies. For example, this work did not focus on the computational efficiency of the modeling and optimization methods used; rather, the focus was on understanding the behavior of the WFLOP problem. Also, turbine positions were allowed to vary continuously, as opposed to most previous work that focuses on a discrete version of the problem. It would be interesting to see if the discretization of the problem, and the enforcement of the 5*D* proximity constraints, affects the density of solutions in different areas of the Pareto set. Finally, in working toward developing formulations, algorithms, and implementations to solve a comprehensive version of the WFLOP, an immediate next step will be the consideration of realistic wind farm terrains, including all the constraints on turbine positions that arise in practice due to environmental considerations, existing infrastructure such as roads, dwellings, transmission lines, and terrain features such as elevation and soil characteristics, among others.

Acknowledgment

The authors would like to thank Hatch, Ltd., for its support during the realization of this project. This work was partially supported by the Natural Sciences and Engineering Research Council of Canada (NSERC), under Grants Nos. CRD-386374-09, DISC-356090-09, and EGP-417630-11. Peter Zhang gratefully acknowledges financial support provided by the Hatch Scholarship for Sustainable Energy Research (2011–2013). Finally, the authors would like to thank the anonymous referees for their valuable comments on earlier versions of this manuscript.

Nomenclature

A = sound attenuation factor
A_{atm} = attenuation factor due to atmospheric absorption
A_{bar} = attenuation factor due to physical barriers
A_{div} = attenuation factor due to geometrical divergence
$A_f(j)$ = A-weighting coefficients to calculate the effective sound level in dBA
A_{gr} = attenuation factor due to ground effects
A_{misc} = attenuation factor due to miscellaneous effects
AEP = annual energy production of a wind farm
$\mathcal{D}$ = set of all possible wind states (speeds, directions)
D_c = directivity correction for a noise source
f = subscript spanning octave band frequencies
L_f = sound pressure level (SPL) at frequency f
L_w = sound power emitted by a source at a given frequency
L_{wA} = A-weighted sound pressure level
p_d = probability of wind state d
P_{tot} = total power extracted from a set of wind turbines
r_r = radius of the wake immediately after the turbine
r_1 = radius of the wake at an arbitrary position downstream of the turbine
SPL = total, effective sound pressure level
u_i = effective wind speed at turbine i, i.e., $u(x_i)$
$u_i(x)$ = effective wind speed at location x due to the i-th turbine
u_{id} = effective wind speed at turbine i for wind state d
$u_{id,\infty}$ = undisturbed wind speed at turbine i for wind state d
u_{ijd} = wind speed at turbine i due to a single wake caused by upstream turbine j for wind state d
u_o = free stream wind speed
u_r = wind speed immediately after the turbine
$u(x)$ = effective wind speed at location x due to n turbines
$\mathcal{U}_{id}$ = set of turbines upstream of turbine i for wind state d
$\mathbf{x}_r$ = vector containing the (continuous) coordinates of the noise receptors in a Cartesian reference frame
$\mathbf{x}_t$ = vector containing the (continuous) coordinates of the turbines in a Cartesian reference frame
z = hub height of the turbine
z_o = surface roughness of the terrain
α = entrainment (wake decay) constant

References

[1] Canadian Wind Energy Association, 2008, "Wind Vision 2025," Canadian Wind Energy Association, Technical Report No. 1.
[2] American Wind Energy Association, 2012, "Industry Statistics," American Wind Energy Association, U.S. Wind Industry Annual, Market Report 2012 No. 1.
[3] Energy Information Administration, 2012, "Annual Energy Review 2011," Office of Energy Statistics, Department of Energy, Technical Report No. DOE/EIA-0384.
[4] Chief Medical Officer of Health (CMOH), 2010, "The Potential Health Impact of Wind Turbines," Ministry of Health and Long-Term Care, Government of Ontario, Canada, Technical Report No. 014894.
[5] Ministry of the Environment, 2008, "Noise Guidelines for Wind Farms," Ministry of the Environment, Government of Canada, Technical Report No. 4709e.
[6] Ministry of the Environment, 2011, "Compliance Protocol for Wind Turbine Noise—Guideline for Acoustic Assessment and Measurement," Ministry of the Environment, Government of Canada, Technical Report No. 8540e.
[7] Mosetti, G., Poloni, C., and Diviacco, B., 1994, "Optimization of Wind Turbine Positioning in Large Wind Farms by Means of a Genetic Algorithm," J. Wind Eng. Ind. Aerodyn., **51**(1), pp. 105–116.
[8] Grady, S., 2005, "Placement of Wind Turbines Using Genetic Algorithms," Renewable Energy, **30**(2), pp. 259–270.

[9] Fagerfjäll, P., 2010, "Optimizing Wind Farm Layouts: More Bang for the Buck Using Mixed Integer Linear Programming," Master's thesis, Chalmers University of Technology, Gothenburg University, Gothenburg, Sweden.
[10] Chowdhury, S., Zhang, J., Messac, A., and Castillo, L., 2011, "Characterizing the Influence of Land Configuration on the Optimal Wind Farm Performance," Proceedings of the ASME 2011 International Design Engineering Technical Conferences & Computers and Information in Engineering Conference, ASME, New York.
[11] Jensen, N., 1983, "A Note on Wind Generator Interaction," Riso National Laboratory, Technical Report No. RISO-M-2411.
[12] Holland, J. H., 1975, *Adaptation in Natural and Artificial Systems*, University of Michigan, Ann Arbour, MI.
[13] Emami, A., and Noghreh, P., 2010, "New Approach on Optimization in Placement of Wind Turbines Within Wind Farm by Genetic Algorithms," Renewable Energy, **35**(7), pp. 1559–1564.
[14] Serrano-González, J., Gonzalez Rodriguez, A. G., Mora, J. C., Santos, J. R., and Payan, M. B., 2010, "Optimization of Wind Farm Turbines Layout Using an Evolutive Algorithm," Renewable Energy, **35**(8), pp. 1671–1681.
[15] Kusiak, A., and Song, Z., 2010, "Design of Wind Farm Layout for Maximum Wind Energy Capture," Renewable Energy, **35**(3), pp. 685–694.
[16] Réthoré, P.-E., Fuglsang, P., Larsen, G. C., Buhl, T., Larsen, T. J., and Madsen, H. A., 2013, "TOPFARM: Multi-Fidelity Optimization of Wind Farms," Wind Energy. Available at: http://onlinelibrary.wiley.com/doi/10.1002/we.1667/abstract.
[17] Saavedra-Moreno, B., Salcedo Sanz, S., Paniagua Tineo, A., Prieto, L., and Portilla Figueras, A., 2011, "Seeding Evolutionary Algorithms With Heuristics for Optimal Wind Turbines Positioning in Wind Farms," Renewable Energy, **36**(11), pp. 2838–2844.
[18] Chowdhury, S., Zhang, J., Messac, A., and Castillo, L., 2012, "Unrestricted Wind Farm Layout Optimization (UWFLO): Investigating Key Factors Influencing the Maximum Power Generation," Renewable Energy, **38**(1), pp. 16–30.
[19] Şişbot, S., Turgut, Ö., Tunç, M., and Çamdali, Ü., 2010, "Optimal Positioning of Wind Turbines on Gökçeada Using Multi-Objective Genetic Algorithm," Wind Energy, **13**(4), pp. 297–306.
[20] Kennedy, J., and Eberhart, R., 1995, "Particle Swarm Optimization," Proceedings of the IEEE International Conference on Neural Networks, IEEE, Vol. 4, pp. 1942–1948.
[21] Wan, C., Wang, J., Yang, G., and Zhang, X., 2010, "Optimal Micro-Siting of Wind Farms by Particle Swarm Optimization," *Advances in Swarm Intelligence*, Vol. 6145 (Lecture Notes in Computer Science), Springer, Berlin, Heidelberg, pp. 198–205.
[22] Bilbao, M., and Alba, E., 2009, "Simulated Annealing for Optimization of Wind Farm Annual Profit," 2nd International Symposium on Logistics and Industrial Informatics, IEEE, pp. 1–5.
[23] Du Pont, B. L., and Cagan, J., 2010, "An Extended Pattern Search Approach to Wind Farm Layout Optimization," Proceedings of the ASME 2010 International Design Engineering Technical Conferences & Computers and Information in Engineering Conference, ASME, New York, Paper No. DETC2010-28748.
[24] Du Pont, B. L., and Cagan, J., 2012, "An Extended Pattern Search Approach to Wind Farm Layout Optimization," ASME J. Mech. Des., **134**(8), p. 081002.
[25] Donovan, S., Nates, G., Waterer, H., and Archer, R., 2008, "Mixed Integer Programming Models for Wind Farm Design," Columbia University, New York. Available at: http://coral.ie.lehigh.edu/~jeff/mip-2008/.
[26] Donovan, S., 2006, "An Improved Mixed Integer Programming Model for Wind Farm Layout Optimisation," Proceedings of the 41st Annual Conference of the Operations Research Society, pp. 143–151.
[27] IBM, 2012, IBM ILOG CPLEX Optimizer.
[28] Turner, S., Romero, D., Zhang, P., Amon, C., and Chan, T., 2014, "A New Mathematical Programming Approach to Optimize Wind Farm Layouts," Renewable Energy, **63**, pp. 674–680.
[29] Zhang, P. Y., Romero, D. A., Beck, J. C., and Amon, C. H., 2013, "Solving Wind Farm Layout Optimization With Mixed and Integer Programming and Constraint Programming," *Integration of AI and OR Techniques in Constraint Programming for Combinatorial Optimization Problems*, C. Gomes, and M. Sellmann, eds., Vol. 7874 (Lecture Notes in Computer Science), Springer, Berlin, Heidelberg, pp. 284–299.
[30] Manwell, J. F., McGowan, J. G., and Rogers, A. L., 2009, "Aerodynamics of Wind Turbines," *Wind Energy Explained*, Wiley, New York, Chap. 3.
[31] Réthoré, P.-E., 2009, "Wind Turbine Wakes in Atmospheric Turbulence," PhD thesis, Aalborg University, Aalborg, Denmark.
[32] International Organization for Standardization, Acoustics—Attenuation of Sound During Propagation Outdoors. Part 2: General Method of Calculation.
[33] Delta Acoustics & Electronics, 2006, "Nord2000—Comprehensive Outdoor Sound Propagation Model. Part 1: Propagation in an Atmosphere Without Significant Refraction," Nordic Noise Group & Nordic Road Directorates, Technical Report No. AV 1849/00.
[34] Delta Acoustics & Electronics, 2009, "Validation of the Nord2000 Propagation Model for Use on Wind Turbine Noise," Energinet, Denmark, Technical Report No. AV 1236/09.
[35] Gandibleux, X., Sevaux, M., Sörensen, K., and T'kindt, V., eds., 2004, *Metaheuristics for Multiobjective Optimisation*, Vol. 535 (Lecture Notes in Economics and Mathematical Systems), Springer, Berlin, Heidelberg.
[36] Zitzler, E., and Thiele, L., 1999, "Multiobjective Evolutionary Algorithms: A Comparative Case Study and the Strength Pareto Approach," IEEE Trans. Evol. Comput., **3**(4), pp. 257–271.
[37] Zitzler, E., Laumanns, M., and Thiele, L., 2001, "SPEA2: Improving the Strength Pareto Evolutionary Algorithm for Multiobjective Optimization," Proceedings of EUROGEN—Evolutionary Methods for Design, Optimisation and Control With Application to Industrial Problems, K. Giannakoglou, D. T. Tsahalis, J. Periaux, and K. D. Papailiou, eds., pp. 95–100.
[38] Srinivas, N., and Deb, K., 1994, "Multiobjective Optimization Using Nondominated Sorting in Genetic Algorithms," Evol. Comput., **2**(3), pp. 221–248.
[39] Deb, K., Pratap, A., Agarwal, S., and Meyarivan, T., 2002, "A Fast and Elitist Multiobjective Genetic Algorithm: NSGA-II," IEEE Trans. Evol. Comput., **6**(2), pp. 182–197.
[40] Zitzler, E., Deb, K., and Thiele, L., 2000, "Comparison of Multiobjective Evolutionary Algorithms: Empirical Results," Evol. Comput., **8**(2), pp. 173–195.
[41] AWS Truepower, 2011, OPENWIND.
[42] AWS Truepower, 2010, "OPENWIND Theoretical Basis and Validation," Albany, NY, Technical Report No. 1.3.
[43] Archer, R., Nates, G., Donovan, S., and Waterer, H., 2011, "Wind Turbine Interference in a Wind Farm Layout Optimization Mixed Integer Linear Programming Model," Wind Eng., **35**(2), pp. 165–175.
[44] Du Pont, B. L., Cagan, J., and Moriarty, P., 2012, "Optimization of Wind Farm Layout and Wind Turbine Geometry Using a Multi-Level Extended Pattern Search Algorithm that Accounts for Variation in Wind Shear Profile Shape," ASME International Design Engineering Technical Conferences & Computers and Information in Engineering Conference, ASME, New York, Paper No. DETC2012-70290.
[45] Chowdhury, S., Messac, A., Zhang, J., Castillo, L., and Lebron, J., 2010, "Optimizing the Unrestricted Placement of Turbines of Differing Rotor Diameters in a Wind Farm for Maximum Power Generation," Proceedings of the ASME 2010 International Design Engineering Technical Conference & Computers and Information in Engineering Conference IDETC/CIE 2010, ASME, New York, pp. 1–16, Paper No. DETC2010-29129.
[46] Dimcev, V., Najdenkoski, K., Stoilkov, V., and Kokolanski, Z., 2011, "Wind Energy Potential Assessment in the Republic of Macedonia," J. Energy Power Eng., **5**(4), pp. 324–330.